



## Phase holdup measurement in a gas–liquid–solid circulating fluidized bed (GLSCFB) riser using electrical resistance tomography and optical fibre probe

S.A. Razzak<sup>a</sup>, S. Barghi<sup>a</sup>, J.-X. Zhu<sup>a,\*</sup>, Y. Mi<sup>b</sup>

<sup>a</sup> Department of Chemical and Biochemical Engineering, University of Western Ontario, 1151 Richmond Street, London, ON, Canada N6A 5B9

<sup>b</sup> En'Urga Inc., 1291-A Cumberland Ave., West Lafayette, IN 47906, USA

### ARTICLE INFO

#### Article history:

Received 20 February 2008

Received in revised form 23 June 2008

Accepted 1 July 2008

#### Keywords:

Electrical resistance tomography

Circulating fluidized bed

Fibre optic

Phase holdup

### ABSTRACT

Phase holdups were measured in the riser section of a gas–liquid–solid circulating fluidized bed (GLSCFB). Electrical resistance tomography (ERT) as a non-invasive imaging technique, pressure transducers (PTs) and fibre optic probes were employed. Water was used as continuous and conductive phase, air as the gas phase and glass beads as solid nonconductive phases. ERT technique is based on conductivity measurement of the continuous phase (water in this study), which provides color-coded cross-sectional view of phases with a frequency of up to 250 images per second. The local conductivity measured by a number of electrodes located at the periphery of the plane was then further converted into a local phase concentration distribution based on Maxwell's relation. The results obtained by PTs, when combined with ERT results, were used to determine gas and solid holdups. Fibre optic probe was also employed to measure gas holdup independently. To measure gas and solid holdup, a model was introduced to exploit the fibre optic data in differentiating gas bubbles from solid particles in the riser. Radial profiles of the phase holdups were determined.

Crown Copyright © 2008 Published by Elsevier B.V. All rights reserved.

### 1. Introduction

Gas–liquid–solid circulating fluidized beds (GLSCFBs) have been widely used in chemical, petrochemical and biochemical and environmental processes, such as hydrogenation, desulfurization, fermentation, due to its efficient mixing, heat and mass transfer capabilities. Most of the studies on gas–liquid–solid fluidization systems have mainly focused on conventional expanded bed regime in the past decades [1]. Therefore a number of theoretical, empirical and semi-empirical models have been developed about hydrodynamics of such systems. The application of these models is limited in GLSCFB. Conventional fluidized beds also suffer from limitations such as liquid and gas velocities, solid particles size, density, etc. In GLSCFB, solid particles are circulated between the riser and the downer at higher velocities compared to conventional fluidized beds, which leads to formation of smaller bubbles and a better contact between phases. GLSCFB also offers great flexibility in terms of solid particles or catalyst regeneration in the downer. In spite of substantial work the hydrodynamics of GLSCFB is not completely understood yet.

Different methods have been employed in the study of hydrodynamics such as direct sampling, optical fibre, electric conductive probe, process tomography, static-pressure, ultrasound and isokinetic separation. Phase holdups as a main parameter was of major concern. Warsito and Fan [2] used electrical capacitance tomography (ECT) to distinguish the three phases qualitatively. Due to the complexity of the systems, different techniques should be applied simultaneously for quantitative measurement of phase holdups.

In this study, electrical resistance tomography (ERT), a newly developed method for the measurement phase holdups, is presented. However ERT cannot measure phase holdups for all the phases, therefore an optical fibre probe and pressure transducers (PTs) are used simultaneously to measure phase holdups for all three phases. In the experiments, water was used as the liquid (continuous and conductive) phase, air as the gas phase and glass beads with 500  $\mu\text{m}$  range as the solid phase. Combination of these measurement techniques provided valuable information about the hydrodynamics of GLSCFB riser. Average phase holdups, and local distribution of phases were obtained and compared with published data wherever applicable.

### 2. Available measurement techniques

Different measurement techniques have been developed to measure phase holdups such as; optical fibre technique, ultrasound

\* Corresponding author. Tel.: +1 519 661 3807; fax: +1 519 661 3498.  
E-mail address: [jzhu@uwo.ca](mailto:jzhu@uwo.ca) (J.-X. Zhu).

**Nomenclature**

$A$	cross-sectional area
$P$	pressure (psia)
$r$	radial position (m)
$R$	radius of the riser (m)
$S$	standard deviation
$U_a$	auxiliary liquid velocity (m/s)
$U_l$	superficial liquid velocity (m/s)
$U_g$	superficial gas velocity (m/s)
$\bar{V}$	average voltage of the signals

*Greek letters*

$\varepsilon$	holdup
$\rho$	density (kg/m <sup>3</sup> )
$\sigma$	conductivity ( $\mu\text{Si}/\text{cm}$ )
$\sigma_i$	local conductivity for single phase ( $\mu\text{Si}/\text{cm}$ )
$\sigma_m$	estimated local conductivity ( $\mu\text{Si}/\text{cm}$ )
$\sigma_0$	local conductivity for mix phases ( $\mu\text{Si}/\text{cm}$ )

*Subscripts*

g	gas phase
l	liquid phase
s	solid phase
ls	liquid–solid phase
gls	gas–liquid–solid phase
bed	fluidized bed

technique, electric conductive probe technique, and process tomographic technique.

Lee and de Lasa [3], de Lasa et al. [4] and Yong and Sang [5] used fibre optic probe to measure the gas holdup directly in a three phase system. A single core silica optical fibre of 400  $\mu\text{m}$  U-shape probe was employed to detect gas bubbles. The gas holdup was determined by measuring the time elapsed by the gas bubbles travelling inside the bed. Air was introduced through large nozzles (0.94 cm) producing large bubbles compared to particles average size (250  $\mu\text{m}$ ). Wang et al. [6] studied bubble behaviour in a fluidized bed using 62.5  $\mu\text{m}$  diameter optical fibre probe. Pipe type distributor was employed to produce large bubbles. Single emitted light beam is sent into the fibre through the fibre coupler and then each beam is reflected at the end of the fibre. Although the application of fibre optic sensor in detection of gas bubbles in a fluidized bed is simple, it is limited by the size of bubbles and not capable of detecting fine bubbles in a dispersed flow regime.

Uchida et al. [7] developed a new technique for solids holdup measurement in a three phase fluidized bed using ultrasonic sound wave. Later, Vatanakul et al. [8,9] used similar concept for flow detection. This technique is based on the change in speed and amplitude of ultrasonic wave incident on a surface. Similar to light beams, when ultrasonic waves strike at the interface between two media, they may be partially/totally reflected, scattered or transmitted. Vatanakul et al. [9] reported that the effects of gas bubbles on sound velocity were contradictory. Some believe that sound velocity is independent of gas holdup whereas others argued that the bubbles could affect sound velocity due to great distortion of ultrasound waves around bubbles [18]. Vatanakul et al. [8] reported that that temperature sensitivity and complicated data analysis were major disadvantages of commercially available ultrasonic instruments.

A dual electrical resistivity probe system was developed by Matsuura and Fan [10] to measure phase holdup and bubble rise velocity in a fluidized bed. The probe was capable of detecting

the difference in conductivity of gas and liquid. The dual conductivity probe consisted of two 0.4 mm diameter stainless steel syringe needles coated with epoxy resin. The vertical distance between the tips was 0.3 mm. The striking bubbles generated signals which were recorded digitally. The average lag time of signals (due to the passing bubbles) were used for calculation of average bubble rise velocity. The technique was claimed to be effective in detecting bubbles as small as 1 mm in size. The method is more applicable to larger bubbles compared to solid particles. The experiments were carried out where the bubbles average size was about 5 mm which was 10–15 times larger than the solids particles used in the experiments. Liang et al. [11,12] used similar setup for gas holdup measurement and a horizontal probe for the measurement of solid holdup in the bubble wake and the emulsion phase. They also measured the solids holdup from the same signals by using the conductivity of the pure liquid as the base line.

Process tomography is an area which has experienced a significant growth over the last 10 years in the study of multiphase flow due to its non-intrusive technique [13]. There are many tomographic techniques, which have been developed in the past 5–10 years and employed in the study of three phase systems such as slurry bubble columns and three phase fluidized beds. However, there are no imaging techniques available for the study of three phase systems in real time [2]. Most of the tomographic techniques such as electrical capacitance tomography, electrical impedance tomography (EIT) or ERT are suitable for two phase systems. George et al. [14] developed a combined system of EIT and gamma-densitometry tomography (GDT) to measure distribution of phases in a vertical three phase flow system simultaneously. Razzak et al. [15] measured phase holdups and velocities in a GLSCFB system by combining ERT and PTs. Warsito and Fan [2] successfully developed a new reconstruction technique for electrical capacitance tomography based on the Hop-field neural network multi-criteria optimization technique (neural network multi-criteria image reconstruction technique, NN-MOIRT). However this imaging technique was useful only in qualitative determination of phases. The application of tomographic technique in the study of multiphase flow systems continues to grow due to its qualitative and quantitative advantages.

### 3. Experimental setup

Schematic diagram of the experimental setup of GLSCFB is shown in Fig. 1. The GLSCFB consists of two main sections, riser and downer, both made of Plexiglas. The riser is 5.97 m tall and 0.0762 m in diameter and the downer is 5.05 m and 0.2 m in diameter. A gas–liquid–solid separator is located at the top of the riser to separate out the solids from the gas and liquid flow and a solids circulation rate measurement device is located near the top of the downer to measure the solids circulation rate.

There are two liquid distributors at the bottom of the riser shown in Fig. 2, the main liquid distributor, made of seven stainless tubes occupying 19.5% of the total riser cross-section and extending 0.2 m into the riser, and the auxiliary liquid distributor, a porous plate with 4.8% opening area at the base of the riser.

The gas distributor shown in Fig. 2 is a tube of 19 mm in diameter and bent in a ring shape of approximately 0.0413 m in diameter, located at 0.34 m above the bottom of the riser. There are 460 small holes of 0.5 mm in diameter on the ring, giving a total opening area of 361 mm<sup>2</sup>, pointing downwards for gas flow. There is also a ring-type liquid distributor in the conical area near the bottom of the downer, which is a tube of 25.4 mm in diameter and bent in a ring shape of approximately 0.114 m in diameter, with 96 small

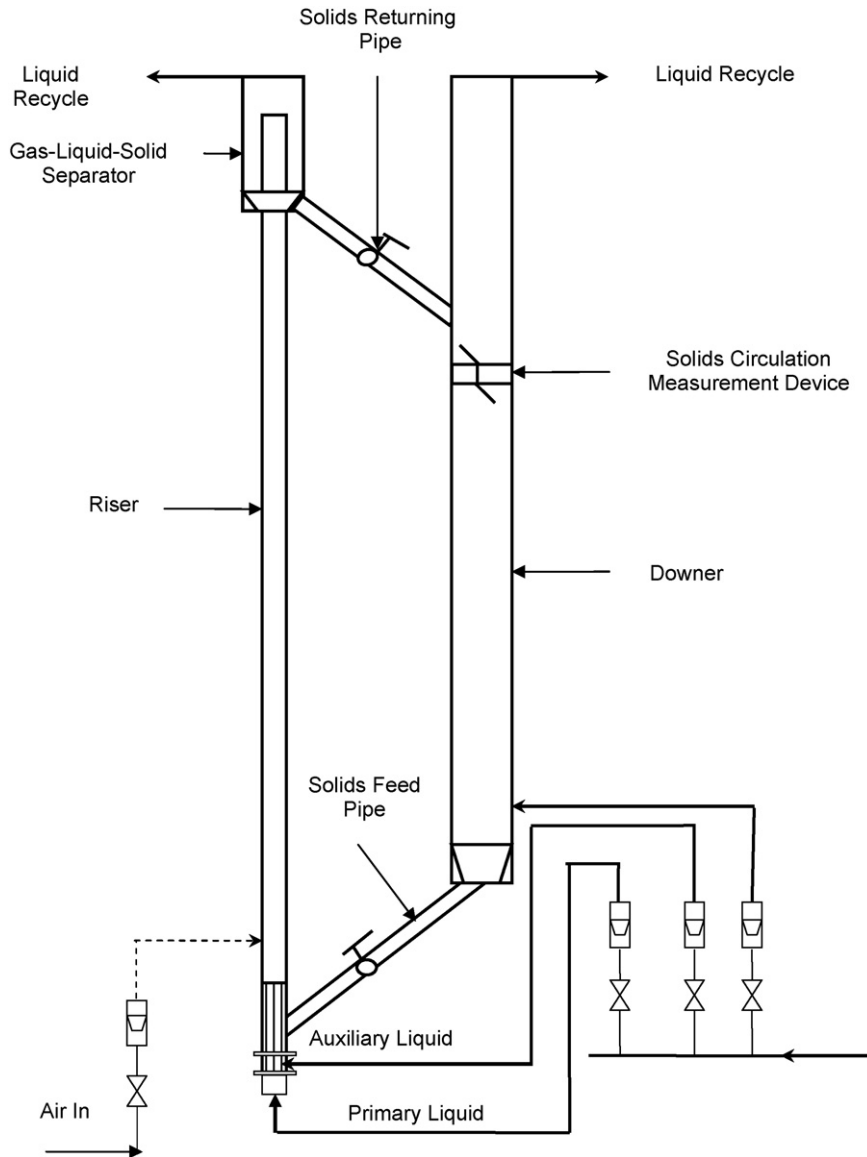


Fig. 1. The schematic diagram of the experimental setup of the GLSCFB system.

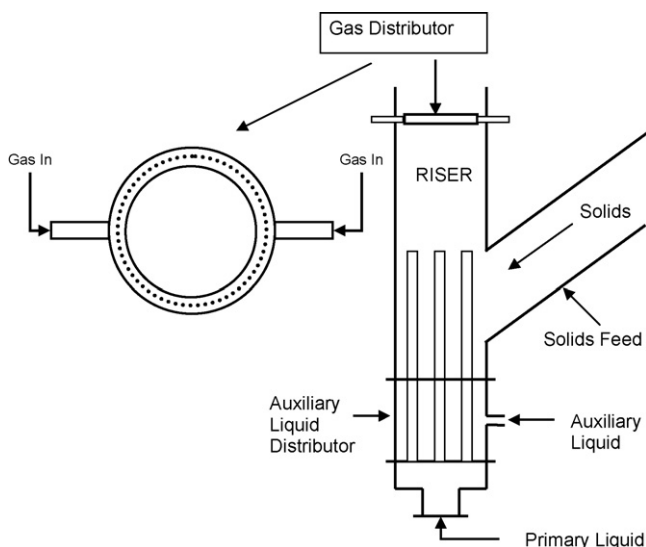


Fig. 2. Schematic diagram of the distributor section in GLSCFB.

holes of 1 mm in diameter on the ring, giving a total opening area of 301 mm<sup>2</sup>, pointing downward for gas flow.

Solid particles are carried up in the riser mainly by the liquid flow, but also assisted by the gas flow. The auxiliary liquid flow is employed to facilitate the flow of solid particles from the downer to the riser, with the main purpose of controlling the solids circulation rate and acting as a non-mechanical valve. The combined effects of both primary and auxiliary liquid flow produce the total liquid flow, which carries the solid particles up in the riser. Air introduced from the gas distributor forms dispersed bubble flow in the riser. Entrained particles in the riser, collected in the gas-liquid-solid separator at the top of the riser, are returned back to the downer after passing through the solids circulation rate measuring device located near the top of the downer. The solids circulation rate measuring device is a special section of the downer located near the top of the downer and just below the solid returning pipe connecting to the riser. A vertical partition plate divides into two halves and there are two half butterfly valves installed at each end of this section. By properly flipping the two half butterfly plates from one side to the other, solids circulated through the system can be accumulated on one side of the measuring section for

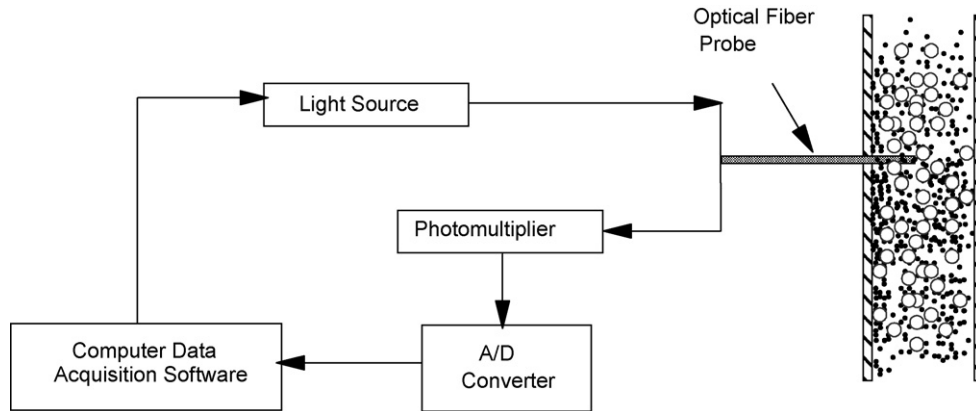


Fig. 3. Optical fibre probe system for gas holdup measurement in GLSCFB riser.

a given time period. All the measurements were carried out in the riser.

#### 4. Optical probe setup and measurement method

Optical fibre probe was successfully employed to measure phase holdups in three phase system by Lee and de Lasa [3]. They used a single core U-shape (radius of the tip = 0.5 mm) optical fibre probe (400  $\mu\text{m}$  in size) to measure gas holdup. Lee and de Lasa [3] measured time average gas holdup from the signal analysis by counting the fraction of time occupied by the gas bubbles. In a similar fashion, Wang et al. [6] used single core 62.5  $\mu\text{m}$  diameter probe to measure gas holdup. They also measured the gas holdup by counting the number of data points occupied by the gas bubble. In those experiments, the average bubble size was about 5 mm which was almost 10–15 times of the average solid particles size.

The optical fibre probes used in the present study were model PV-5, produced by the Institute of Process Engineering, Chinese Academy of Sciences, capable of measuring solids concentration in three phase fluidized beds. Details of the optical fibre probes system are shown schematically in Figs. 3 and 4. They consist of both light emitting and receiving quartz fibres, arranged in an alternating array, corresponding to emitting and receiving layers of fibres as shown in Fig. 3. The diameter of the probe is approximately 4 mm and contains approximately 8000 emitting and receiving quartz fibres with a diameter of 15  $\mu\text{m}$  each. These fibres are arranged in an alternating array, corresponding to emitting and receiving layers of fibres, within a 1.5 mm<sup>2</sup> area at the centre of the probe tip. Their small size does not significantly disturb the overall flow struc-

ture. The results were not significantly influenced by temperature, humidity, electrostatics and electromagnetic fields. In order to prevent particles from occupying the blind zone, a Plexiglas cover of 0.2 mm was placed over the probe tip.

The received light reflected by the particles and gas bubbles was multiplied by the photo-multiplier and converted into voltage signals. The voltage signals were further amplified and fed into a computer. The high voltage adjustment is used to adjust the upper measuring limit. There is also a zero voltage potentiometer, which produces a zero output signal by adjusting the appropriate signal intensity. In order to obtain more accurate representation of radial solids concentration profiles, three measurement ports were installed around the periphery of the column to measure the solids concentration. The sampling time was 10 s with a frequency of 2 kHz. To ensure the validity and repeatability of sampled signals, at least three samples were taken at each measuring position for each run.

In this study, water was used as the liquid and continuous phase. Typical offset was initially set at zero for the liquid output voltage. Consequently water does not produce any voltage output signal. However in the presence of the solid particles in the liquid–solid two phase system, signals were detected. Since the solid particles moved randomly, a fluctuating signal was produced as shown in Fig. 5. Fig. 5 shows a segment of the data collected in 1 s. This situation changes from location to location not only under the same condition but also for different operating parameters. The average voltage of the signal produced of this particular case was 1.334 V

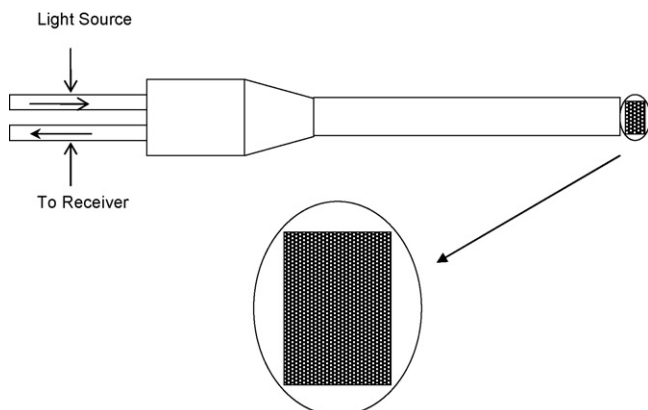


Fig. 4. Schematic diagram of phase holdups measuring optical fibre probe.

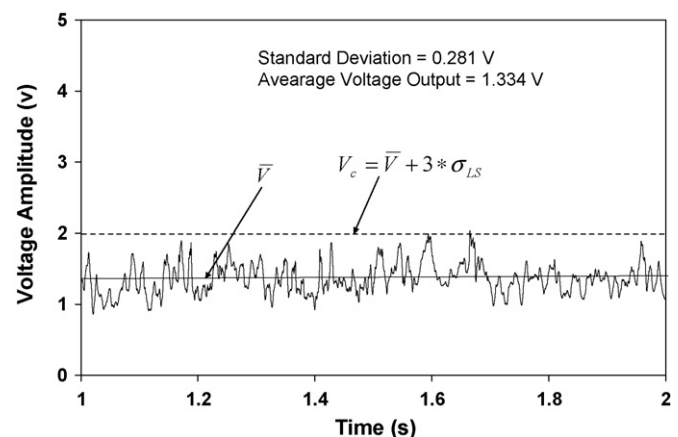


Fig. 5. The typical voltage output signal produce by optical fibre probe for liquid–solid system in GLSCFB riser.

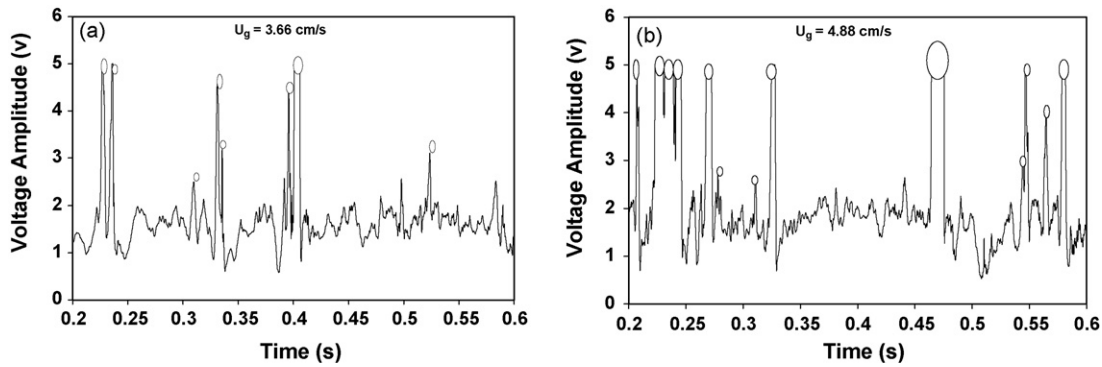


Fig. 6. Voltage output signal produced by optical fibre probe for gas-liquid-solid system in GLSCFB riser for two different superficial gas velocities.

with a standard deviation of 0.241 V. The output voltage in the presence of bubbles was larger. The analysis of the data under different conditions showed that the critical voltage for the detection of bubbles was the average voltage  $\pm 3$  times the standard deviation:

$$V_c = \bar{V} + 3\sigma_{LS} \quad (1)$$

where  $\bar{V}$  is the average voltage of the signals and  $\sigma_{LS}$  is the standard deviation for the liquid-solid system. Therefore, any voltage out of this range is the indication of a gas bubble.

Gas holdup measurement in gas-liquid-solid systems is really challenging when the gas is in dispersed phase and bubbles are much larger than solid particles. In the present experiments average bubble size lies in between five and twenty times of the solid particles size in a wide operation ranges. Bubble sizes are reduced when the liquid velocity is sufficiently high and grow at lower liquid velocities. Fig. 6 shows the signals produced in the gas-liquid-solid system for two particular operating cases,  $U_g = 3.66$  cm/s and 4.88 cm/s with the same superficial liquid velocity. It can be observed that bubble produces distinctively bigger signals than those of solid particles. Signals associated with large bubbles can be easily distinguished and differentiated from the rest as shown in Fig. 6. The amplitude of the small bubbles' signals was quite small and quite close to that of solid particles, which made it difficult to differentiate this bubbles. However, the contribution of the small bubbles to the average gas holdup was small and was thus ignored. It is to mention that signal amplitude and bubbling frequency increased with increasing gas velocity.

The signals obtained in the GLSCFB were similar to the liquid-solids system. However the detailed review of these signals was useful in developing an empirical model to detect the bubbles which were at least three times larger than the average diameter of solid particles. The proposed model used to measure the gas holdup is

$$V_c = \bar{V}_{LS} + \left( \frac{\bar{V}_{gls} - \bar{V}_{LS}}{\bar{V}_{LS}} \right) \sigma_{LS} + 4\sigma_{LS} \quad (2)$$

where  $\bar{V}_{LS}$  is the average voltage of the signals produced from the liquid-solid system,  $\bar{V}_{gls}$  is average voltage of the signals in the GLSCFB, and  $\sigma_{LS}$  is the standard deviation for liquid-solid system.

The multiplying factor  $(\bar{V}_{gls} - \bar{V}_{LS})/\bar{V}_{LS}$  used in the equation is to find out the exact critical voltage above which all the data points represent the gas bubbles. Any change in the gas and liquid flow rates can affect the size and number of gas bubbles. Fig. 7 shows critical voltage measurement used to measure gas holdups using optical fibre probe in GLSCFB riser. The average voltage of the signals in the GLSCFB riser is influenced by the bubbles size and numbers. The dimensionless multiplying factor was then adjusted to measure the particular critical voltage. The time averaged local gas

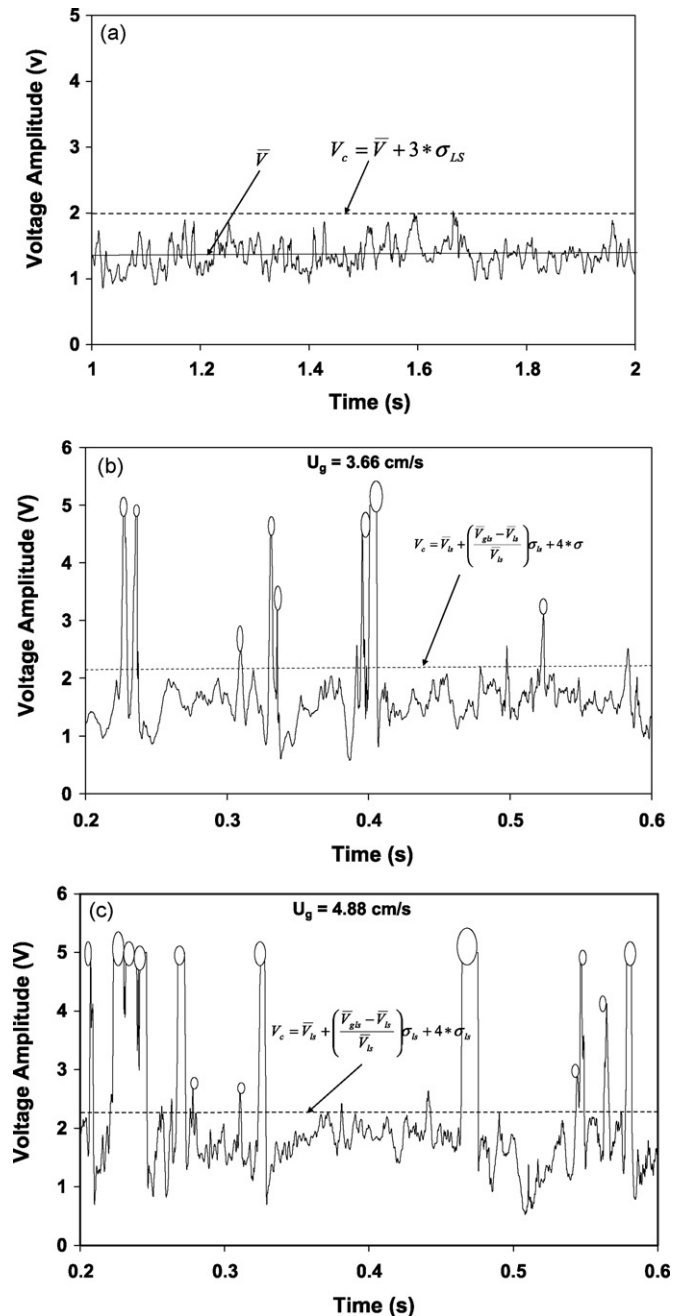


Fig. 7. Critical voltage measurement used to measure gas holdups using optical fibre probe in GLSCFB riser.

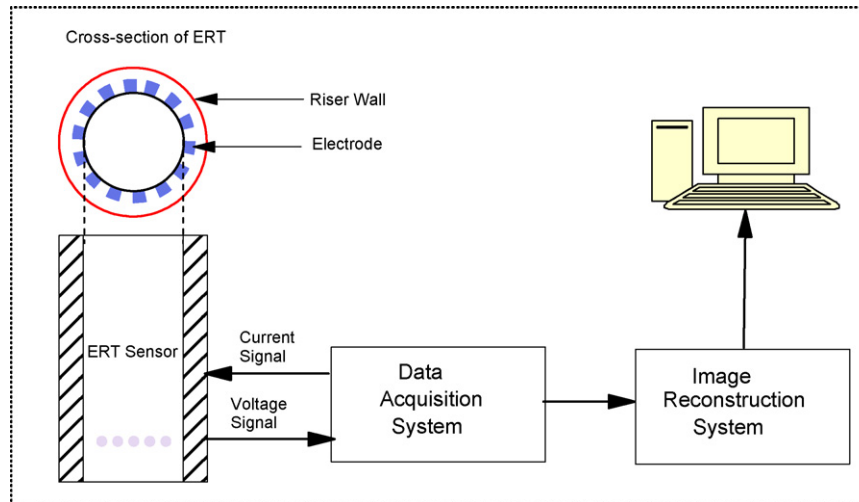


Fig. 8. Schematic diagram of the measurement principle of ERT for GLSCFB system.

holdup then can be obtained by counting the number of data points occupied by the gas bubbles above the critical voltage threshold.

### 5. ERT setup and measurement method

ERT is a non-intrusive soft-field tomographic system, by which the phase holdups and velocity distributions can be measured. In principle, both qualitative and quantitative measurements estimated on the basis of local conductivity and/or resistivity of different phases in a multiphase flow system measured by a number of sensors installed at the periphery of the ERT system. A typical measurement setup illustrated in Fig. 8, comprises an ERT sensor, a data acquisition system and a personal computer. Data acquisition system connected with the electrodes in ERT sensor is responsible for setting currents and reading voltages.

The ERT system used in the present study (EnERT) manufactured by En'Urga Inc. The ERT sensor has two sets of signal cable connectors as well as one for a ground cable. The inner diameter of the sensor section is built equal to the inner diameter of the riser so that the sensors can be lined up with the riser. The liner of the sensor section supports three planes of electrodes. Sixteen electrodes equally spaced on the first plane provide the voltage signals for reconstructing fine phase distributions, primarily for the distribution of solids and gas (nonconductive phase) holdups. Each of the two other planes contains eight electrodes, used to provide voltage signals for reconstructing coarse phase distributions. Cross-correlating between the latter two planes yields estimations of local or zone-averaged phase propagation velocities. For the current study, the sensor section is installed at the height of 2.02 m.

The electronic circuit of the EnERT has two additional cables, a power cable and a data acquisition cable. The data acquisition cable is a standard cable from National Instruments (NI) used to link the NI connectors on the electronic box and the data acquisition board in the computer.

AC currents were applied to the electrodes. For each driving current, the ERT measures the electrical potential distribution through the electrodes flush mounted on the wall. Fig. 9 shows the current injection strategy through the pair-electrodes attached on the boundary of the ERT sensor for voltage measurements. During each operating frame, multiple driving currents are sequentially fed into a pair of neighbouring electrodes. The voltages are measured on all other electrodes except the current injecting electrodes pair. The way in which the driving pair is switched and the voltage measurements are collected varies. With the applied current source,

electrical potential distributions are generated within the fluids and the wall. Electronic circuits captured voltages between the electrodes and send them to a PC-based data acquisition system. The saved data is processed with an image reconstruction algorithm which provides the phase distributions occurred in the experiments.

In the presents study, water is used as a conductive and continuous phase. On the other hand gas and solids both are nonconductive and dispersed phases. Proper calibration is crucial to get the actual phase distributions as it reduces the measurement error in converting the conductivity data to phase concentrations. Prior to each experiment, calibration was done by adjusting the conductivity of the liquid with adding sodium chloride.

A reconstruction algorithm was used to determine the internal resistivity and the phase holdups within the GLSCFB riser from the acquired data. With input values of the electrical potentials

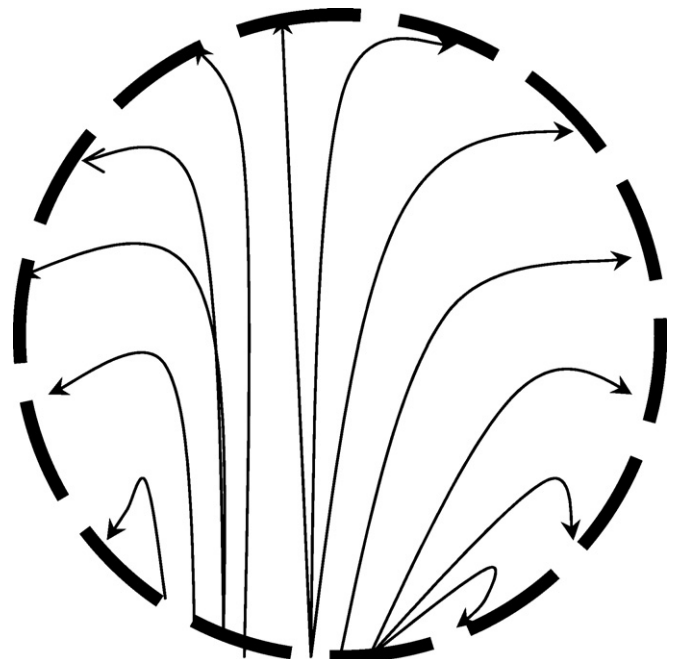


Fig. 9. Current injection strategy through pair-electrodes attached on the boundary of the ERT sensor for voltage measurements.

and currents, the local conductivity (or resistivity) of the mixture can be reconstructed through a state-of-the-art optimization algorithm. The algorithms reside in the personal computer connected with data acquisition system and can be used on an off-line basis. Algorithm produces images quantitatively and depicting the conductivity or phase holdups for each pixel. A 2D finite element method (FEM) model was employed for the phase holdup measurements due to its speed, overall simplicity and accuracy. Most of the process vessels have circular cross-section, which facilitate finite element meshing process [16]. Forward problem is solved using the FEM-solver and the resultant set of voltages then compared with the boundary voltages measured from the data acquisition system. The least square error between the two sets of voltages then calculated and compared with the predefined error. If the least square error is less than the predefined error then iteration process is stopped. If it is greater than the error then the resistivity of each element is updated via Newton–Raphson technique and then is fed to the solver for further iteration.

The final conductivity distribution is then further converted into the local phase concentration distribution based on Maxwell's relation. The ERT system obtains data at 250 (500 optional) frames per second. For a steady-state condition, the data can be collected for a certain period of time. Before the conversion, the local conductivity is first non-dimensionalized using the equation:

$$\sigma = \frac{\sigma_m - \sigma_1}{\sigma_0 - \sigma_1} \quad (3)$$

where  $\sigma_m$  denotes the estimated local conductivity,  $\sigma_1$  denotes the local conductivity when the pipe is full of single liquid phase and  $\sigma_0$  denotes the local conductivity when the pipe is full of gas or solid or both phases. The conductivity of the first phase ( $\sigma_1$ ) can be found easily with available commercial conductivity meters, while the local estimated mixture conductivity ( $\sigma_m$ ) is determined from the pixel conductivity of ERT image data. The Maxwell relation is employed to convert the local conductivity to the local gas and solid holdups [15]:

$$\varepsilon = 1 - \frac{3\sigma^*}{2 + \sigma^*} \quad (4)$$

## 6. Pressure transducers and measurement method

PTs (OMEGA-PX61) were used to measure average solids phase holdup by measuring pressure gradient in the riser. This method calculated solids holdup on particular measurement location which will be used for the verification the cross-sectional average solids holdup measured by ERT. Calibrated PTs were installed at six axial locations on the riser column wall, which were connected to the computer via an A/D converter. For all experiments, the pressure signals were sampled with a frequency of 1000 Hz for a total of 20 s. The two PTs located closest to the ERT measurement sensor were used to provide the local pressure data across the sensor section.

Pressure drop in the riser is mainly due to liquid and solid static head, plus the friction at the wall. Since the fluidization velocity in GLSCFB is not very high compared to gas–solid fluidization, the wall friction is not significant. The measured pressure drop per unit length of the bed is therefore proportional to bed density,  $\rho_{bed}$ , i.e.:

$$\frac{\Delta P}{\Delta Z} = \rho_{bed}g = (\varepsilon_s \rho_s + \varepsilon_l \rho_l + \varepsilon_g \rho)g \quad (5)$$

where  $\Delta P$  is the pressure drop across the measured section of the bed and  $\Delta Z$  is the height of the measured section. Since,  $\rho_g$  is about two orders of magnitude smaller than either  $\rho_l$  or  $\rho_s$ , the gas effect is negligible and thus ignored. From ERT data the average conductive

liquid phase holdup can be obtained, which can be put into the above Eq. (5), to obtain the solid holdup:

$$\varepsilon_s \cong \frac{(\Delta P / (\Delta Z g)) - \varepsilon_l \rho_l}{\rho_s} \quad (6)$$

## 7. Phase holdups measurement

Little work has been done in the study of local phase holdups in multiphase flow systems, particularly in GLSCFBs due to the complexity of the available measurement techniques. In this study new approach was considered to measure the local phase holdups by using the combination of ERT and optical fibre probe data. Seven radial positions (distributed radially, centred at  $r/R=0, 0.2034, 0.492, 0.6396, 0.7615, 0.8641, \text{ and } 0.9518$ ) were considered to measure gas and solids holdups. These locations were considered for dividing the cross-sectional area of the GLSCFB riser in six equal zones to measure zone and time based average solid and gas holdups.

As discussed, the ERT system can provide phase distributions of a multiphase flow by differentiating between the conductive and nonconductive phases. Therefore, when the nonconductive phase consists of two phases, e.g. gas and solid phases as in this study, it would be impossible to determine the holdups of the two phases separately at particular location. However if the holdup of one of the phases can be determined by another method, the complete distribution of phases can be estimated. Therefore fibre optic probes were employed to measure the gas holdup. The combination of ERT and fibre optic data successfully revealed the phase holdups of all the phases at different locations.

Fig. 10 shows the radial distributions of gas, solids and liquid phase holdups at different superficial gas and liquid velocities where superficial liquid velocity  $U_l = 5.6$  cm/s and auxiliary liquid velocity  $U_a = 1.4$  cm/s in the GLSCFB riser. All measurements were carried out at an axial location of  $H = 2.02$  m above the distributor. Solids holdup initially remained constant at the central location and started to increase radially toward the wall. Opposite trend was observed for the gas holdup as it sharply decreased in wall region. Similar results were reported by Yang et al. [17] and Vatanakul et al. [8].

Optical fibre probe data in a particular radial location was used to calculate the time averaged cross-sectional phase holdup, from which the area averaged cross-sectional phase holdup is calculated by

$$\bar{\varepsilon} = \frac{2}{R^2} \int_0^R \varepsilon r \, dr \quad (7)$$

Whereas in ERT, phase holdup was measured in six equal zones with the same area. Therefore, cross-sectional average phase holdup was calculated from the time average data captured using ERT by

$$\bar{\varepsilon} = \frac{\sum_{i=1}^6 \varepsilon_i A_i}{A} \quad (8)$$

Cross-sectional average phase holdups are depicted in Fig. 11. Cross-sectional average solids holdup sharply decreases with the increase of superficial liquid velocity. Cross-sectional average of solids holdup increased with the increase of superficial gas velocity. A slight increase of solids circulation rates, thus the solids holdup, was observed after introducing gas to the system. Similar observation was reported by Vatanakul et al. [9] and Razzak et al. [15]. This trend disappeared with the increases of superficial liquid velocity. Cross-sectional average of solid holdup also verified with the data measured by PTs. PTs measured solids holdup around the measurement locations and it can be assumed that

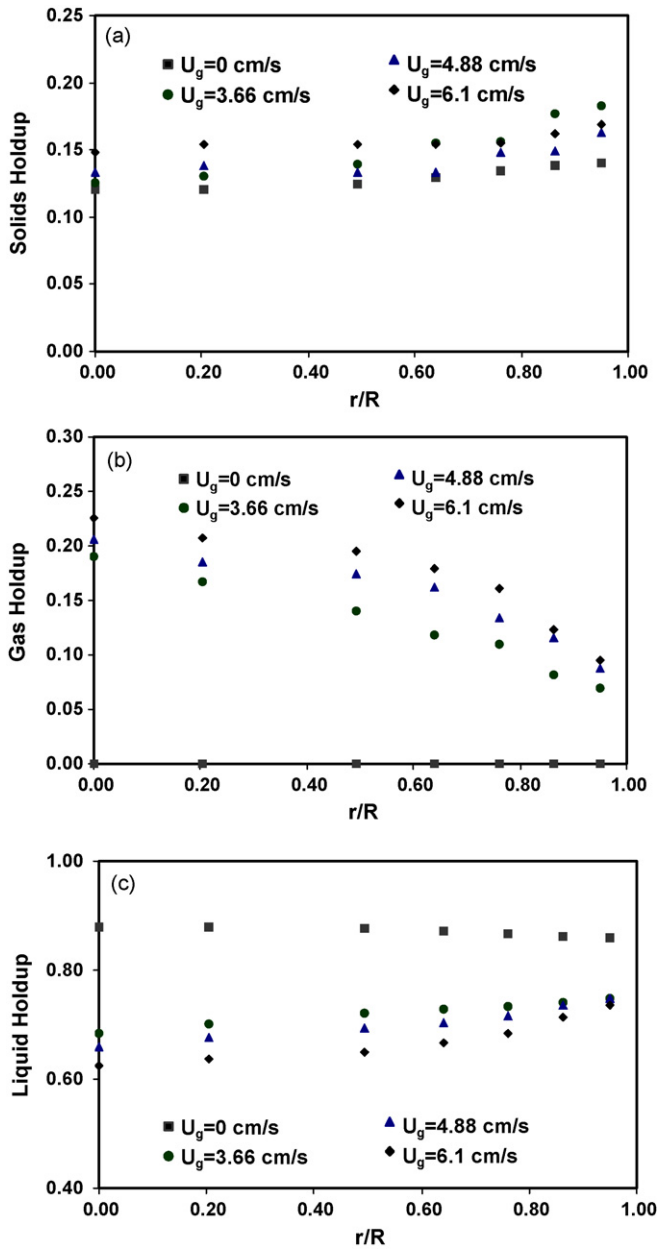


**Fig. 10.** Radial distribution of gas, liquid, and solids holdup measured for different superficial gas velocity at superficial liquid velocity  $U_l = 5.6$  cm/s and auxiliary liquid velocity  $U_a = 1.4$  in a GLSCFB riser using the combination of ERT and optical probe.

cross-sectional average solids holdup will not vary within short distances. Table 1 shows the average solids holdup measured with both techniques.

The error was less than 5% as shown in Table 1. The data provided by PTs are averaged values which were assumed to be constant, however due to the distance between the PT and ERT sensors there

**Table 1**

Comparison between the average solids holdup values obtained with different methods

$U_l$ (cm/s)	ERT and OP	ERT and PT	% Error
35	0.0281	0.0267	4.98
22.4	0.0502	0.0484	3.58
11.2	0.0941	0.0915	2.79
8.4	0.0981	0.0962	1.95
5.6	0.1522	0.1448	4.87

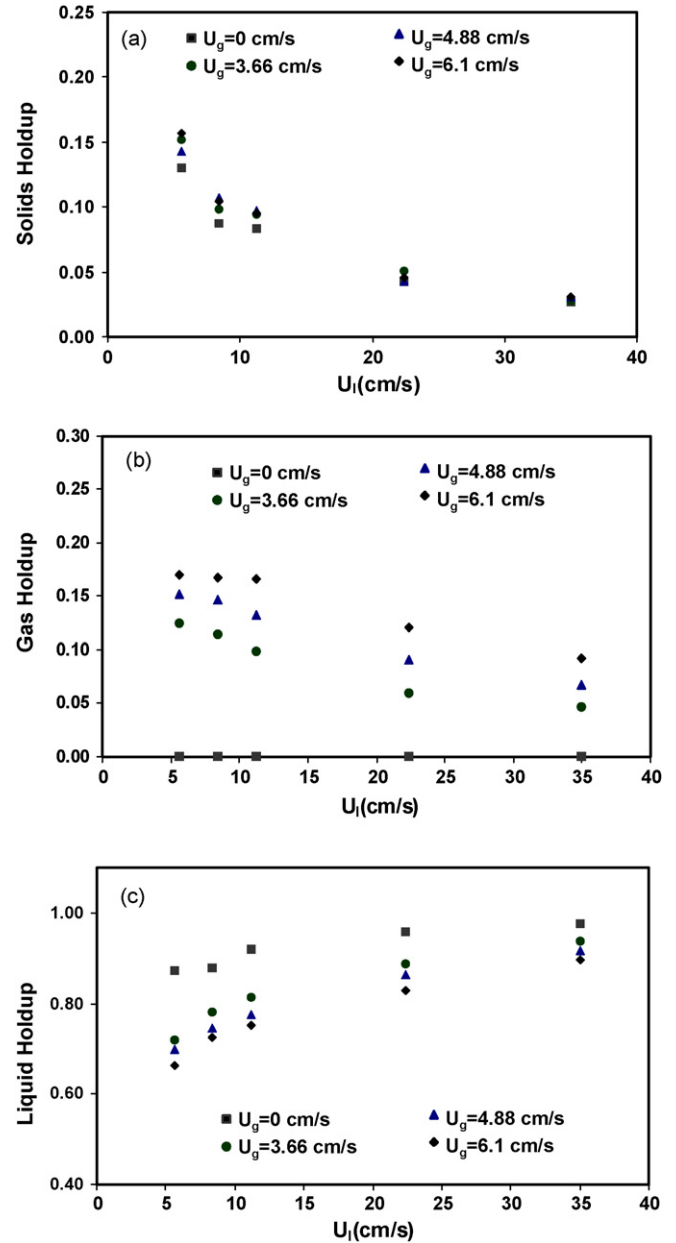


**Fig. 11.** Cross-sectional average gas, liquid, and solids holdup measured varying different superficial liquid velocity for different superficial gas velocity at auxiliary liquid velocity  $U_a = 1.4$  in a GLSCFB riser using the combination of ERT and optical probe.

would be small changes. Major part of the errors may be attributed to these changes.

Cross-sectional average of gas holdup increases with the increases of superficial gas velocity and it goes down with the increases of superficial liquid velocity. On the other hand the remaining phase (liquid phase) has shown the reverse trend.

## 8. Conclusions

Measurement techniques of phase holdups in three phase systems were reviewed in this paper. The new ERT technique was employed to measure the local distribution of phase holdup in a three phase circulating fluidized bed. In spite of being an advanced technology, ERT application in three phase systems is limited to the measurement of conductive phase only, which makes it impossible



to differentiate between the other nonconductive phases, e.g. solids and gas in this study. A new method was developed to determine the phase holdups of all phases for a better understanding of hydrodynamics in GLSCFB systems. Combining the advanced technology of ERT and optical fibre probe revealed the phase holdups in GLSCFB riser quantitatively. Optical fibre probe was capable of measuring gas holdup, which was one of the nonconductive phases. Combination of both technologies successfully measured three phases separately.

Radial distribution of phase holdups showed that the solid holdup was lower in the central region and increased radially toward the wall region, while opposite trend was observed for the gas holdup. Cross-sectional average of gas holdup increased with the increase of superficial gas velocity and it decreased with the increases of superficial liquid velocity. Both ERT and OP and ERT and PT have shown a good agreement with little percentage error.

### Acknowledgements

The authors would like to acknowledge the Natural Science and Engineering Research Council of Canada for financial support and the Canada Foundation of Innovation for the infrastructure fund that was used to purchase the ERT.

### References

- [1] K. Muroyama, L.S. Fan, Fundamental of gas–liquid–solid fluidization, *AIChE J.* 40 (1985) 83–92.
- [2] W. Warsito, L.-S. Fan, ECT imaging of three-phase fluidized bed based on three-phase capacitance model, *Chem. Eng. Sci.* 58 (2003) 823–832.
- [3] S.L.P. Lee, H.I. de Lasa, Phase holdups in three-phase fluidized beds, *AIChE J.* 8 (1987) 1359–1370.
- [4] H.I. de Lasa, S.L.P. Lee, M.A. Bergougnou, Bubble measurement in three-phase fluidized beds using a U-shaped optical fiber, *Can. J. Chem. Eng.* 62 (1984) 165–176.
- [5] H.Y. Yong, D.K. Sang, Bubble characteristics in the radial direction of three-phase fluidized beds, *AIChE J.* 34 (1988) 2069–2072.
- [6] T. Wang, J. Wang, Y. Weigu, J. Yong, Experimental study on gas-holdup and gas–liquid interfacial area in TPCFBs, *Chem. Eng. Commun.* 187 (2001) 251–263.
- [7] S. Uchida, S. Okamura, T. Katsumata, Measurement of longitudinal distribution of solids holdup in a three-phase fluidized bed but ultrasonic technique, *Can. J. Chem. Eng.* 67 (1989) 166–176.
- [8] M. Vatanakul, Y. Zheng, M. Couturier, Ultrasonic technique for measuring phase holdups in multiphase systems, *Chem. Eng. Commun.* 192 (2005) 630–646.
- [9] M. Vatanakul, Y. Zheng, M. Couturier, Flow characterization of a three-phase circulating fluidized bed using ultrasonic technique, *Can. J. Chem. Eng.* 81 (2003) 1121–1129.
- [10] A. Matsuura, L.-S. Fan, Distribution of bubble properties in a gas–liquid–solid fluidized, *AIChE J.* 30 (1984) 894–903.
- [11] W. Liang, Q. Wu, Z. Yu, Y. Jin, Z. Wang, Hydrodynamics of a gas–liquid–solid three phase circulating fluidized bed, *Can. J. Chem. Eng.* 73 (1995) 656–681.
- [12] W. Liang, Z. Yu, Y. Jin, Z. Wang, Q. Wu, The phase holdups in a gas–liquid–solid circulating fluidized bed, *Chem. Eng. J.* 58 (1995) 259–264.
- [13] Y. Wu, H. Li, M. Wang, R.A. Williams, Characterization of air–water two-phase vertical flow by using electrical resistance imaging, *Can. J. Chem. Eng.* 83 (2005) 37–41.
- [14] D.L. George, K.A. Shollenberger, J.R. Torczynski, T.J. O' Hern, S.L. Ceccio, Three-phase material distribution measurement in a vertical flow using gamma-densitometry tomography and electrical-impedance tomography, *Int. J. Multiphase Flow* 27 (2001) 1903–1930.
- [15] S.A. Razzak, S. Barghi, J.-X. Zhu, Electrical resistance tomography for flow characterization of a gas–liquid–solid three-phase circulating fluidized bed, *Chem. Eng. Sci.* 62 (2007) 7253–7263.
- [16] F. Dickin, M. Wang, Electrical resistance tomography for process applications, *Meas. Sci. Technol.* 7 (1996) 247–260.
- [17] W.G. Yang, J.F. Wang, W. Chen, Y. Jin, Liquid-phase flow structure and backmixing characteristics of gas–liquid–solid three phase circulating fluidized beds, *Chem. Eng. Sci.* 54 (1999) 5293–5298.
- [18] Y. Zheng, Ultrasound measurement of two or three phase flow detection, *Can. J. Chem. Eng.* 81 (2003) 268–270.